Journal of Peptide Science
J. Pept. Sci. 2008; **14**: 383–388
Published online 11 December 2007 in Wiley InterScience (www.interscience.wiley.com). DOI: 10.1002/psc.980

JOURNAL OF PEPTIDE SCIENCE

Membrane-bound peptides from V-ATPase subunit *a* do not interact with an indole-type inhibitor‡

RENSKE W. HESSELINK,[a,b §] ALEXANDER FEDOROV,[a] MARCUS A. HEMMINGA[b]* and MANUEL PRIETO[a]

[a] Centro de Química-Física Molecular, Instituto Superior Técnico, Lisbon, Portugal
[b] Laboratory of Biophysics, Wageningen University, Wageningen, The Netherlands

Received 9 July 2007; *Revised 3 October 2007*; *Accepted 22 October 2007*

Abstract: The V-ATPases are ATP-dependent proton pumps, found in virtually all cells, responsible for acidification of organelles and energizing of plasma membranes. Its role in diseases, such as osteoporosis and metastatic cancer, makes the V-ATPase a potential drug target. Short synthetic peptides that are presented here mimic the 7th transmembrane domain (TM7) of subunit *a* (Vph1p) of *Saccharomyces cerevisiae* V-ATPase, an essential part of the membrane-bound V_O domain, where proton translocation takes place. The peptides adopt a transmembrane configuration only in membranes containing anionic lipids, stressing the importance of strong interfacial anchoring by the flanking lysines. Peptide P1, which contains the essential arginine R735, is monomeric, whereas peptide P2, which lacks this extra charge, tends to aggregate in the membrane. SB 242784, which is a highly potent inhibitor of V-ATPase, does not show any interaction with the peptides, indicating that TM7 alone is not sufficient for inhibitor binding. Copyright © 2007 European Peptide Society and John Wiley & Sons, Ltd.

Keywords: yeast; V-ATPase (Vph1p); transmembrane helix 7; subunit *a*; transmembrane peptides; time-resolved fluorescence; FRET

INTRODUCTION

The vacuolar H^+-ATPases, or V-ATPases, are ATP-dependent proton pumps found in virtually all cells. They hydrolyse ATP, and use the released energy to pump protons across a membrane. The protons cross the membrane via the membrane-bound V_O domain. This domain contains the subunits *a*, *d* and *e*, which are part of the stator of the molecular motor, and the proteolipid subunits *c*, *c′* and *c″* that make up the rotor [1]. V-ATPases are implicated in a variety of disease processes, including osteoporosis [2] and tumour metastasis [3], and are therefore potential drug targets. Various inhibitors of the enzyme are known, of which the macrolide antibiotics bafilomycin and concanamycin are the most potent, with IC_{50}-values in the low nanomolar range [4]. Since these macrolides inhibit all V-ATPases in different cell types, they are highly poisonous and inappropriate for medicinal use.

Novel derivatives of bafilomycin have been synthesized, which maintain a high inhibitory activity toward V-ATPases and exhibit a high selectivity for the osteoclast form of the enzyme [5,6]. The most promising of these compounds is (2Z,4E)-5-(5,6-dichloro-2-indolyl)-2-methoxy-*N*-(1,2,2,6,6-pentamethylpiperidin-4-yl)-2,4-pentadienamide (SB 242 784) (Figure 1). The chemical structure of this inhibitor is based on the key structural features of bafilomycin linked to an indole ring, and it has an IC_{50}-value for osteoclast V-ATPase of 29 nM [2]. SB 242 784 is also extremely effective in preventing bone loss in ovariectomized rats [7], making this inhibitor a promising candidate for osteoporosis treatment. Little is known about the precise binding site and mechanism of action of inhibitor SB 242 784, although it has been suggested that it binds to the membrane-bound V_O domain [8]. Recently, spin-labelled derivatives of SB 242 784 have been studied by ESR [9]. From this study it was possible to acquire information about the location in the membrane of the piperidine ring where the nitroxide label was inserted. In another study, the interaction of the indole class of V-ATPase inhibitors with lipid bilayers was examined [10]. Fluorescence and ESR studies, combined with site-directed mutagenesis, have shown that the proteolipid subunits contain a major part of the inhibitor binding site [8,11]. However, the finding that the inhibitor has different binding constants for V-ATPase isoforms varying only in subunit *a* strongly suggests that this subunit forms part of the inhibitor binding site as well [5]. In addition, a recent study using high-resolution NMR spectroscopy proposes that a hinge-type movement of the 7th transmembrane segment (TM7) of subunit *a* causes an opening and closing of the cytoplasmic proton hemi-channel to enable proton translocation. Therefore, inhibitors that bind to the cytoplasmic loop segment could rigidify it and thereby potentially disable the translocation of protons [12].

* Correspondence to: Marcus A. Hemminga, Laboratory of Biophysics, Wageningen University, Dreijenlaan 3, 6703 HA Wageningen, The Netherlands; e-mail: marcus.hemminga@wur.nl
‡ This article is part of the Special Issue of the Journal of Peptide Science entitled "2nd workshop on biophysics of membrane-active peptides".
§ Present Address: Institute of Membrane and Systems Biology, Faculty of Biological Sciences, University of Leeds, Leeds, LS2 9JT, UK.

IHTIEFCLNCVSHTASYLRLWALSLAHAQLSSVLWTM
TM7

KKSHTASYL**R**LWALSLAHAQLSSKK
P1

KKSHTASYL**H**LWALSLAHAQLSSKK
P2

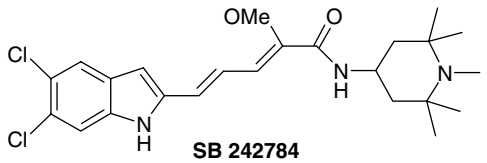

SB 242784

Figure 1 Sequences of V-ATPase subunit *a* residues I720–G760 and of the peptides P1 and P2 that are derived from this sequence. The 7th transmembrane helix (TM7) from subunit *a* (Vph1p) of *Saccharomyces cerevisiae* V-ATPase that runs from V727 to T752 [13–16] is underlined. The structure of the V-ATPase inhibitor SB 242 784 is shown at the bottom.

In this study, small synthetic peptides P1 and P2 are used to mimic TM7 of subunit *a* (Vph1p) of *Saccharomyces cerevisiae* V-ATPase that is essential for proton translocation (Figure 1) [17]. This study parallels a similar study that was carried out to the site of action of inhibitor SB 242 784 to the putative 4th transmembrane segment of subunit *c* using fluorescence spectroscopy [18]. Peptides P1 and P2 contain a tryptophan residue, making it possible to study inhibitor binding by Förster (or fluorescence) resonance energy transfer (FRET).

MATERIALS AND METHODS

Chemicals

1,2-Dioleoyl-*sn*-glycero-3-phosphocholine (DOPC, 18 : 1PC), 1,2-dierucoyl-*sn*-glycero-3-phosphocholine (DEuPC, 22 : 1PC), and 1,2-dioleoyl-*sn*-glycero-3-[phospho-*rac*-(1-glycerol)] (DOPG, 18 : 1PG), were obtained from Avanti Polar Lipids (Birmingham, AL). Inhibitor SB 242 784 (Figure 1) was synthesized as described before [5,6]. Fine chemicals were obtained from Merck (Darmstadt, Germany), except for TFA, which was from Aldrich (St. Louis, MO), and TFE, which was from Acros Organics (Geel, Belgium). All materials were used without further purification.

Peptide Synthesis and Design

The peptides P1 and P2 (Figure 1) were produced on solid support using continuous flow chemistry by Pepceuticals Ltd., Leicester, UK and used without further purification. The final purity was tested by HPLC and mass spectrometry, and was above 90% in all cases.

Peptide P1 contains 21 residues from TM7, including R735 the only subunit *a* residue essential for proton translocation [13]. To study the role of this arginine in more detail, it has been mutated into a histidine in peptide P2. The residues involved in these mutations are shown in bold in Figure 1. Both peptides contain a tryptophan residue (W737 in the native sequence) that is used to study the peptides by fluorescence spectroscopy.

On both sides of the peptide two lysines are added. This approach is frequently used in studies of membrane-bound peptides, as lysines are known to increase solubility, stabilize membrane insertion by interaction with anionic lipid headgroups, promote a transmembrane configuration and minimize aggregation [19].

Peptide Reconstitution in Lipid Vesicles

The peptides were dissolved directly in methanol; alternatively, they were dissolved in a small amount of TFA, which was evaporated under a stream of nitrogen gas, and subsequently dissolved in TFE. The desired amounts of peptide stock solution, lipids in chloroform (DOPC or DEuPC, with or without 20 mole% DOPG) and, if required, inhibitor SB 242 784 in ethanol were mixed and dried under a stream of nitrogen gas. Last traces of organic solvent were evaporated under vacuum for at least 3 h. The 4 : 1 (mol/mol) mixed lipid systems are indicated as DOPC/DOPG and DEuPC/DOPG. After addition of buffer (10 mM Tris, pH = 7.4) and three cycles of vortexing, freezing and thawing, crude multilamellar vesicles were obtained.

In all experiments, the lipid concentration varied from 0.34 to 2.5 mM, and the peptide concentration from 2.0 to 29 μM. The effective peptide concentration (i.e. the amount of peptide per volume of membrane) did not exceed 15 mM (corresponding to a lipid to peptide molar ratio of 85), to keep the system sufficiently diluted.

Absorption and Fluorescence Spectroscopy

Absorption spectra were obtained using a Shimadzu UV-3101PC spectrophotometer (Shimadzu Schweiz, Reinach, Switzerland). The spectra were corrected for light scattering [20].

Steady-state fluorescence spectra were measured on an SLM-Aminco 8100 Series 2 spectrofluorimeter (Rochester, NY; with double excitation and emission monochromators, MC400) in a right-angle geometry. The light-source was a 450-W Xe arc lamp and a Rhodamine B quantum counter solution was used for reference. Spectral bandwidths varied from 2 to 16 nm.

Time-resolved fluorescence decay measurements of tryptophan were carried out at room temperature with a time-correlated single-photon counting system [21]. Excitation of tryptophan was at 295 nm and emission was monitored at 340 nm. Data analysis was carried out using a non-linear, least-squares iterative convolution method [22]. The tryptophan fluorescence decay was described by a sum of exponentials. For the FRET analysis, we used the lifetime-weighted quantum yield, which is proportional to the area under the decay curve. This lifetime-weighted quantum yield was also used in the evaluation of the self-quenching efficiency. However, the mean or average lifetime, was the one considered in the Stern-Volmer plots (both self-quenching and acrylamide quenching, for details see Ref. 23).

DOI: 10.1002/psc

Acrylamide Quenching

Aliquots of 4 μl of a 3 M stock solution were added to a 700 μl sample, until a final concentration of 0.13 M acrylamide was reached. The fluorescence spectra were measured as soon as there was no decrease in intensity. Data were analysed according to the Stern-Volmer equation [23].

Self Quenching

In the self-quenching experiments, the effective peptide concentration in mixed DOPC/DOPG vesicles was varied. Effective peptide concentrations were calculated assuming the volume of one lipid molecule (either DOPC or DOPG) of 1296 $Å^3$ [24].

Inhibitor Binding

In the experiments with SB 242 784, the inhibitor was co-solubilized with peptides P1 or P2 in DOPC/DOPG bilayers to obtain a homogeneous distribution of the inhibitors in the membrane. A lipid concentration of 2.5 mM was used to achieve high partitioning of the inhibitor into the membrane. The energy transfer efficiency in the FRET experiments was obtained from the time-resolved measurements [23]. The FRET data were analysed using an analytical model for energy transfer for the case of randomly distributed donors and acceptors in different planes [25]. The inhibitor concentrations ranged from 1.8 to 39 μM. The most concentrated samples had an effective inhibitor concentration of 20 mM (about 64 lipid molecules per inhibitor).

RESULTS AND DISCUSSION

Effects of Bilayer Thickness and Interfacial Anchoring

The first goal of our research is to find a suitable model membrane system to embed peptides P1 and P2. For this we used lipid systems of DOPC and DEuPC, and these lipids mixed with DOPG. The fluorescence emission spectra of peptide P2 in the pure lipid systems are red-shifted compared to the mixed lipid systems with DOPG. This indicates that part of the peptides is not associated with the membrane in a transmembrane configuration, and is most probably adsorbed at the interface or dissolved in the water phase (data not shown). Clearly, the favourable interactions between the negatively charged DOPG headgroups in the mixed lipid system and the positively charged lysines that flank the peptides on both sides are needed to anchor the peptides in the membrane. The spectrum of peptide P2 in DEuPC, with an emission maximum close to 350 nm, is similar to that of peptide P2 dissolved in water (data not shown), indicating that in this case a major fraction of the peptide is not incorporated into the membrane.

As compared to DOPC/DOPG bilayers, in the thicker bilayer system DEuPC/DOPG the emission spectrum of peptide P2 shifts approximately 7 nm to the blue end. Apparently the peptide is anchored in the membrane so stably that it is able to stay in a transmembrane configuration even when it is subjected to some negative hydrophobic mismatch; probably this is possible through snorkelling of the lysines [26]. Because DEuPC forms thicker membranes, the tryptophan residue will be buried more deeply in this system and the emission spectrum will be blue-shifted compared to the DOPC/DOPG system. The results for peptide P1 are similar (data not shown).

Acrylamide-quenching experiments confirm these results. Figure 2 shows the Stern-Volmer plots for acrylamide quenching of peptide P2 reconstituted into the different membrane systems. In all cases, the accessibility of the tryptophan of peptide P2 is reduced as compared to the quenching of water-dissolved peptide, where the usual static component of quenching is also apparent. The tryptophan residue buried in the thick DEuPC/DOPG membrane is almost inaccessible to the water-soluble quencher as expressed by the Stern-Volmer constant $K_{SV} = 2.3\ M^{-1}$, while in the thinner DOPC/DOPG membrane it is somewhat more accessible ($K_{SV} = 5.3\ M^{-1}$). In DEuPC an even higher K_{SV} value is expected as compared to the binary lipid systems with DOPG, and this is in fact observed ($K_{SV} = 7.6\ M^{-1}$).

The fluorescence and quenching data are in agreement with a transmembrane conformation of peptides P1 and P2 in DOPC/DOPG bilayers, in accordance with previous studies on these peptides [17]. DEuPC is used for comparison with DOPC to analyse the transmembrane configuration of the peptides, in samples with an increased membrane thickness. However, using DEuPC/DOPG bilayers would result in a negative hydrophobic mismatch that could incorrectly affect our further analyses. The DOPC/DOPG system would provide a better match with the peptide length. In addition, this bilayer system is closer to the native system

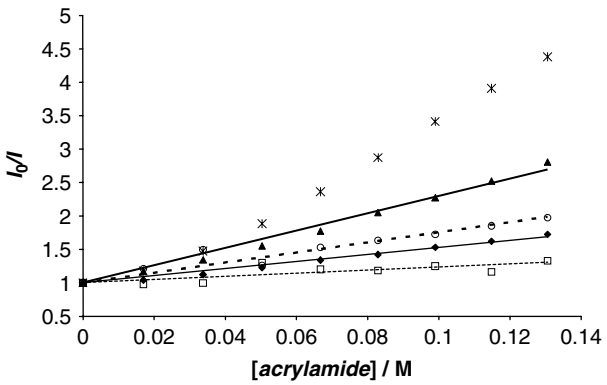

Figure 2 Stern-Volmer plots for acrylamide quenching of peptide P2, reconstituted into vesicles composed of DOPC (thick line, ▲), DEuPC (thick dotted line, ○), DOPC/DOPG (thin line, ♦) and DEuPC/DOPG (thin dotted line, □). For comparison the Stern-Volmer plot for acrylamide quenching of water-dissolved peptide P2 (*) is also shown.

DOI: 10.1002/psc

and this lipid system will be used to study peptide aggregation and interaction effects with inhibitor SB 242 784.

Peptide Aggregation

To examine the state of the peptides P1 and P2 in DOPC/DOPG bilayers, self-quenching experiments were carried out (Figure 3). Peptide P1 does not show any dynamic self-quenching over the full concentration range studied, indicated by a constant lifetime-weighted quantum yield of 2.4 ns. Peptide P2 self-quenching is seen in up to an effective peptide concentration of 8 mM. At higher peptide concentrations the lifetimes tend to level off, and such a type of deviation is ascribed to extensive peptide aggregation. From the fit in the low concentration range, a value for the bimolecular quenching constant of 2.0×10^{10} M^{-1} s^{-1} was obtained using the experimentally determined average lifetime of 4.5 ns, determined in the diluted regime.

The bimolecular quenching constant allows the estimation of the molecular diffusion coefficient using the Smoluchowski equation [27]. Taking into account a collisional radius of tryptophan of 5 Å [28], a diffusion coefficient of 1.0×10^{-5} cm^2 s^{-1} is obtained. This value is much higher (about three orders of magnitude) than the diffusion coefficient for single peptides in a lipid bilayer reported in the literature [28,29]. This can be explained by peptide aggregation/segregation of the peptide into a limited area of the membrane. This would lead to a higher effective peptide concentration, and therefore the values of the bimolecular quenching constant and the diffusion coefficient, obtained assuming a random distribution of peptides in the membrane, are overestimated. Aggregation of the peptide would in fact decrease the diffusion coefficient, but this is overcome by the significant increase in effective concentration.

For peptide P1 no self-quenching is observed in this concentration range, and thus it can be concluded that it is randomly distributed in the membrane, essentially as monomers. The difference between the two peptides might be caused by the extra charge on peptide P1. This peptide contains an arginine located approximately 7 Å from the centre of the lipid bilayer [17]. This residue is most likely protonated and positively charged; to accommodate this charge in the hydrophobic core of the membrane, it might be snorkelling, thereby positioning its charged group in the interfacial region of the membrane [17]. This extra charge, which is missing in peptide P2, since the histidine is not charged at the conditions used, causes an extra repulsion between the peptides and thus less aggregation.

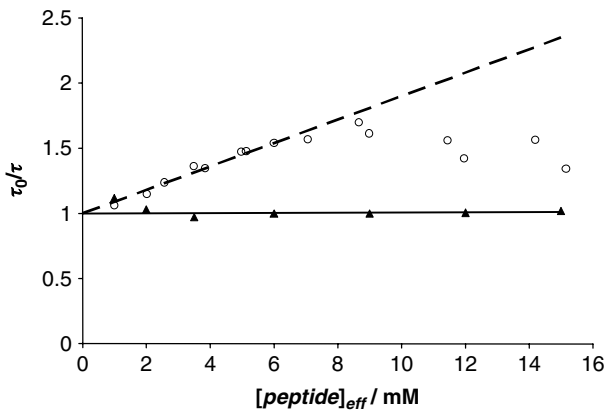

Figure 3 Transient state Stern-Volmer plots, describing self-quenching of peptide P1 (solid line, ▲) and peptide P2 (dotted line, ○) in DOPOC/DOPC vesicles. The lines are fits of the Stern-Volmer equation [23] to the data.

Interaction with Inhibitor SB 242 784

On the basis of key structural features of bafilomycin, a group of indole-based inhibitors has been designed [2]; the binding of the most potent of these, inhibitor SB 242 784, to peptides P1 and P2 is studied here. Since inhibitor SB 242 784 contains an indole ring involved in extensive conjugation, it has a strong absorption, with an extinction coefficient of 4.1×10^4 M^{-1} cm^{-1} at 365 nm (F. Fernandes, private communication), and emission centred around 440 nm. Therefore, energy transfer from the Trp in peptide P1 or P2 to inhibitor SB 242 784 is an efficient process that can provide information on the lateral distribution of inhibitor SB 242 784 around the peptides.

The FRET experiments were carried out at a constant effective concentration of the donor (peptide P1 or P2) of 2 mM in DOPC/DOPG vesicles. The effective concentration of the acceptor inhibitor SB 242 784 (i.e. the amount of inhibitor per membrane volume) was varied from 0 to 19 mM. Figure 4 shows the FRET efficiencies from peptides P1 and P2 to inhibitor SB 242 784. The efficiencies are calculated from lifetime measurements. The experimental data points are compared to a theoretical curve for energy transfer to randomly distributed acceptors [25]. In this calculation, the Trp donors are positioned at 4 Å from the centre of the membrane as determined by parallax analysis [17]. It is assumed that each donor can transfer its energy to acceptors randomly distributed in two planes, 14 Å from the centre of the bilayer, which is the approximate position for inhibitor SB 242 784 [10]. It is assumed that 93% of the SB 242 784 molecules partitions into the membranes at a lipid concentration of 2.5 mM, based on the partition coefficient for the inhibitor in this lipid system [10].

For peptide P1, a very good fit of the theoretical curve for randomly distributed acceptors to the experimental data was obtained. Therefore, it can be concluded that there is no specific interaction between peptide P1 and inhibitor SB 242 784. This means that the inhibitor is randomly distributed around the peptide, and does not prefer to be in close proximity to it. For peptide

DOI: 10.1002/psc

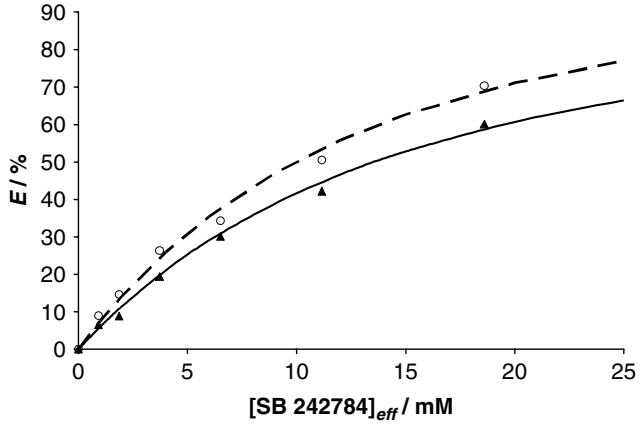

Figure 4 FRET efficiency from peptide P1 (○) and peptide P2 (▲) to inhibitor SB 242 784 calculated from the lifetimes versus the effective inhibitor (acceptor) concentration in DOPC/DOPG vesicles. The dashed and solid lines represent the calculated FRET efficiencies for a random distribution of acceptors [25]. The dashed line takes into account an exclusion radius of 15 Å based on an α-helical transmembrane peptide. The solid line is calculated for an exclusion radius of 25 Å, to simulate aggregation of the peptides.

P2, all experimental FRET efficiencies are lower than expected for a random distribution of acceptors around the donors (Figure 4). This could be related to the fact that peptide P2 aggregates, contrary to peptide P1, as seen in the self-quenching experiments (Figure 3). This would imply an increased exclusion radius for energy transfer. To simulate this situation a second theoretical curve is calculated, based on an exclusion radius of 25 Å, which fits the experimental data well (Figure 4). Clearly, there is no indication for a specific binding of inhibitor SB 242 784 to peptide P2 either.

For both peptides the distribution of inhibitors around them is random, and in addition for peptide P2 there is evidence for peptide aggregation, due to the larger exclusion radius for energy transfer. This raises the question whether subunit *a* TM7 is involved in inhibitor binding at all. The inhibitors used in this study might bind only to subunit *c*, which would explain why no interaction is observed here. Recent studies with bafilomycin and concanamycin point to the proteolipid subunits as binding site for these inhibitors [8,30–32]; Bowman *et al.* [30,31] propose a binding pocket within the four subunit *c* helices, in which case the inhibitors would not be in contact with subunit *a* at all.

For inhibitor SB 242 784, on the other hand, much less evidence exists for binding to subunit *c* [8]. This inhibitor shows a different affinity for V-ATPases only differing in their subunit *a* isoform, strongly suggesting a role for this subunit in binding. Fluorescence quenching experiments on the whole V_O domain and its purified subunits also indicate that subunit *a* is involved in inhibitor binding [11]. TM7 is the most likely candidate, since this helix contains the most important residues for activity and is in contact with the proteolipids. The data presented here show that TM7 alone is not sufficient to effect binding of the inhibitor, and that other parts of subunit *a* or the proteolipid subunits are needed as well.

Acknowledgements

This work was supported by contract no. QLG-CT-2000-01801 of the European Commission (MIVase – New Therapeutic Approaches to Osteoporosis: targeting the osteoclast V-ATPase). M.A.H. and M.P. are members of the COST D22 Action 'Protein-Lipid Interactions' of the European Union.

REFERENCES

1. Sambade M, Kane PM. The yeast vacuolar proton-translocating ATPase contains a subunit homologous to the *Manduca sexta* and bovine *e* subunits that is essential for function. *J. Biol. Chem.* 2004; **279**: 17361–17365.
2. Farina C, Gagliardi S, Nadler G, Morvan M, Parini C, Belfiore P, Visentin L, Gowen M. Novel bone antiresorptive agents that selectively inhibit the osteoclast V-H^+-ATPase. *Farmaco* 2001; **56**: 113–116.
3. Martinez-Zaguilan R, Lynch R, Martinez G, Gillies R. Vacuolar type H^+-ATPases are functionally expressed in plasma membranes of human tumor cells. *Am. J. Physiol.* 1993; **265**: C1015–C1029.
4. Dröse S, Boddien C, Gassel M, Ingenhorst G, Zeeck A, Altendorf K. Semisynthetic derivatives of concanamycin A and C, as inhibitors of V- and P-type ATPases: structure-activity investigations and developments of photoaffinity probes. *Biochemistry* 2001; **40**: 12816–12825.
5. Gagliardi S, Nadler G, Consolandi E, Parini C, Morvan M, Legave M-N, Belfiore P, Zocchetti A, Clarke GD, James I, Nambi P, Gowen M, Farina C. 5-(5,6-Dichloro-2-indolyl)-2-methoxy-2,4-pentadienamides: Novel and selective inhibitors of the vacuolar H^+-ATPase of osteoclasts with bone antiresorptive activity. *J. Med. Chem.* 1998; **41**: 1568–1573.
6. Nadler G, Morvan M, Delimoge I, Belfiore P, Zocchetti A, James I, Zembryki D, Lee-Rycakzewski E, Parini C, Consolandi E, Gagliardi S, Farina C. (2Z,4E)-5-(5,6-Dichloro-2-indolyl)-2-methoxy-N-(1,2,2,6,6-pentamethylpiperidin-4-YL)-2,4-pentadienamide, a novel, potent and selective inhibitor of the osteoclast V-ATPase. *Bioorg. Med. Chem. Lett.* 1998; **8**: 3621–3626.
7. Visentin L, Dodds RA, Valente M, Misiano P, Bradbeer JN, Oneta S, Liang X, Gowen M, Farina C. A selective inhibitor of the osteoclastic V-H^+-ATPase prevents bone loss in both thyroparathyroidectomized and ovariectomized rats. *J. Clin. Invest.* 2000; **106**: 309–318.
8. Páli T, Whyteside G, Dixon N, Kee TP, Ball S, Harrison MA, Findlay JBC, Finbow ME, Marsh D. Interaction of inhibitors of the vacuolar H^+-ATPase with the transmembrane V_o-sector. *Biochemistry* 2004; **43**: 12297–12305.
9. Dixon N, Pali T, Kee TP, Marsh D. Spin-labelled vacuolar-ATPase inhibitors in lipid membranes. *Biochim. Biophys. Acta* 2004; **1665**: 177–183.
10. Fernandes F, Loura L, Koehorst RBM, Dixon N, Kee TP, Hemminga MA, Prieto M. Interaction of the indole class of V-ATPase inhibitors with lipid bilayers. *Biochemistry* 2006; **45**: 5271–5279.
11. Whyteside G, Meek PJ, Ball SK, Dixon N, Finbow ME, Kee TP, Findlay JBC, Harrison MA. Concanamycin and indolyl pentadieneamide inhibitors of the vacuolar H^+-ATPase bind with high

affinity to the purified proteolipid subunit of the membrane domain. *Biochemistry* 2005; **44**: 15024–15031.
12. Duarte AMS, De Jong ER, Wechselberger R, Van Mierlo CPM, Hemminga MA. Segment TM7 from the cytoplasmic hemi-channel from $V_O - H^+$-V-ATPase includes a flexible region that has a potential role in proton translocation. *Biochim. Biophys. Acta* 2007; **1768**: 2263–2270.
13. Kawasaki-Nishi S, Nishi T, Forgac M. Arg-735 of the 100-kDa subunit a of the yeast V-ATPase is essential for proton translocation. *Proc. Natl. Acad. Sci. U.S.A.* 2001; **98**: 12397–12402.
14. Kawasaki-Nishi S, Nishi T, Forgac M. Interacting helical surfaces of the transmembrane segments of subunits a and c' of the yeast V-ATPase defined by disulfide-mediated cross-linking. *J. Biol. Chem.* 2003; **278**: 41908–41913.
15. Kawasaki-Nishi S, Nishi T, Forgac M. Proton translocation driven by ATP hydrolysis in V-ATPases. *FEBS Lett.* 2003; **545**: 76–85.
16. Nishi T, Forgac M. The vacuolar (H^+)-ATPases–Nature's most versatile proton pumps. *Nat. Rev. Mol. Cell Biol.* 2002; **3**: 94–103.
17. Hesselink RW, Koehorst RBM, Nazarov PV, Hemminga MA. Membrane-bound peptides mimicking transmembrane Vph1p helix 7 of yeast V-ATPase: A spectroscopic and polarity mismatch study. *Biochim. Biophys. Acta* 2005; **1716**: 137–145.
18. Fernandes F, Loura LMS, Fedorov A, Dixon N, Kee TP, Prieto M, Hemminga MA. Binding assays of inhibitors towards selected V-ATPase domains. *Biochim. Biophys. Acta* 2006; **1758**: 1777–1786.
19. de Planque MRR, Killian JA. Protein-lipid interactions studied with designed transmembrane peptides: Role of hydrophobic matching and interfacial anchoring. *Mol. Membr. Biol.* 2003; **20**: 271–284.
20. Castanho MARB, Santos NC, Loura LMS. Separating the turbidity spectra of vesicles from the absorption spectra of membrane probes and other chromophores. *Eur. Biophys. J.* 1997; **26**: 253–259.
21. Loura LMS, Fedorov A, Prieto M. Membrane probe distribution heterogeneity: a resonance energy transfer study. *J. Phys. Chem. B* 2000; **104**: 6920–6931.
22. Marquardt DW. An algorithm for least-squares estimation of nonlinear parameters. *J. Soc. Ind. Appl. Math.* 1963; **11**: 431–441.
23. Lakowicz JR. *Principles of Fluorescence Spectroscopy*, 2nd edn. Kluwer Academic/Plenum Publishers: New York, 1999.
24. Wiener MC, White SH. Structure of a fluid dioleoylphosphatidylcholine bilayer determined by joint refinement of X-ray and neutron-diffraction data. 3. Complete structure. *Biophys. J.* 1992; **61**: 437–447.
25. Fernandes F, Loura LMS, Koehorst RBM, Spruijt RB, Hemminga MA, Fedorov A, Prieto M. Quantification of protein-lipid selectivity using FRET: Application to the M13 major coat protein. *Biophys. J.* 2004; **87**: 344–352.
26. Strandberg E, Killian JA. Snorkeling of lysine side chains in transmembrane helices: How easy can it get? *FEBS Lett.* 2003; **544**: 69–73.
27. Umberger JQ, Lamer VK. The kinetics of diffusion-controlled molecular and ionic reactions in solution as determined by measurements of the quenching of fluorescence. *J. Am. Chem. Soc.* 1945; **67**: 1099–1109.
28. de Almeida RFM, Loura LMS, Prieto M, Watts A, Fedorov A, Barrantes FJ. Cholesterol modulates the organization of the γM4 transmembrane domain of the muscle nicotinic acetylcholine receptor. *Biophys. J.* 2004; **86**: 2261–2272.
29. Fernandes F, Loura LMS, Prieto M, Koehorst R, Spruijt RB, Hemminga MA. Dependence of M13 major coat protein oligomerization and lateral segregation on bilayer composition. *Biophys. J.* 2003; **85**: 2430–2441.
30. Bowman BJ, Bowman EJ. Mutations in subunit c of the vacuolar ATPase confer resistance to bafilomycin and identify a conserved antibiotic binding site. *J. Biol. Chem.* 2002; **277**: 3965–3972.
31. Bowman EJ, Graham LA, Stevens TH, Bowman BJ. The bafilomycin/concanamycin binding site in subunit c of the V-ATPase from *Neurospora crassa* and *Saccharomyces cerevisiae*. *J. Biol. Chem.* 2004; **279**: 33131–33138.
32. Huss M, Ingenhorst G, Konig S, Gassel M, Drose S, Zeeck A, Altendorf K, Wieczorek H. Concanamycin a, the specific inhibitor of V-ATPases, binds to the V_o subunit c. *J. Biol. Chem.* 2002; **277**: 40544–40548.

DOI: 10.1002/psc